Line of Sight and Alternative Representations of Aberrations of the Eye

Stanley A. Klein, PhD; Daniel D. Garcia, PhD

ABSTRACT

Several methods for representing pupil plane aberrations based on wavefront height, slope, and curvature are discussed. The choice of reference axis and reference surface is shown to strongly affect the appearance of the representation. Special attention will be paid to the use of the line of sight (the line from the fixation point to the center of the pupil) as the reference axis. We show that the line of sight is ambiguous and does not determine the amount of prism in the wavefront. [*J Refract Surg* 2000;16:S630-S635]

In recent years there has been an explosion of activity measuring aberrations of the eye. One of the goals of this activity is to develop methods for predicting visual performance. It is not yet clear how to do that prediction. It is likely that different aspects of visual performance will require different ways of viewing the aberrations. This paper examines and compares five graphical representations of the aberration data (Figs 1, 2, 4, 5, and 6). The advantages and disadvantages of the different displays will be discussed.

There are two domains for specifying aberrations: the retinal plane and the pupil plane. In the retinal plane, aberrations are represented by the point spread function and its Fourier transform, the modulation transfer function. These retinal representations are sufficiently familiar that they will not be examined here. Rather, we examine pupil plane representations of aberrations. Pupil plane aberrations have special relevance to the task of correcting the aberrations using deformable mirrors, refractive surgery, and contact lenses. The most common pupil plane representation is the wavefront height. We compare several additional representations, including wavefront curvature and the pupil point spread function (pPSF), based on wavefront slope.

We also discuss possible reference axes and reference surfaces for measuring and displaying aberrations. We examine how the appearance of the aberrations in different representations depends strongly on the choices made for the reference axis and reference surface. How these choices can affect estimates of optimal image quality will be considered. The suggestion that the line of sight be used as the reference axis is discussed. We argue that the line of sight is ambiguous and does not determine the amount of prism in the wavefront.

WAVEFRONTS ANALYZED

Two examples of aberrations are examined. The first example is the wavefront aberration found and plotted by Walsh, Charman, and Howland[8] using the objective aberroscope for their subject PD. It is specified by the following Taylor expansion:

$$W(x, y) = -.0033x^3 - .0279x^2y - .0454xy^2 + .0138y^3 + .0141x^4 + .0121x^3y + .0304x^2y^2 + .0161x^3y + .0126y^4 \quad (1)$$

Distances (x, y) are measured in mm and the wavefront, W, is measured in microns. Walsh and colleagues removed all terms below third order (the terms able to be corrected by a sphero-cylindrical lens) when they reported their data.

The second example that we will examine has a wavefront given by:

$$W(x, y) = 2\exp(-((x - 1)^2 + y^2)/2) - 2\exp(-1/2)\ \mu m \quad (2)$$

This wavefront is a symmetric Gaussian with a 1 mm standard deviation, shifted by 1 mm to the right. This wavefront was chosen to simulate a mild keratoconic distortion with peak curvature of

From the School of Optometry, University of California, Berkeley, CA (Klein) and the Computer Science Division, University of California, Berkeley, CA (Garcia).

Published in part in the February, 2000 Technical Digest of the Optical Society of America, and reprinted here with permission of the Optical Society of America.

Correspondence: Stanley A. Klein, PhD, School of Optometry, University of California, Berkeley, CA 94720. Tel: 510.643.8670; Fax: 510.643.5109; E-mail: klein@spectacle.berkeley.edu

2 diopters (500 mm radius of curvature of the wavefront). A more typical keratoconic distortion would have a peak power of 20 D rather than 2 D. An aberration of 2 D is in the range of aberrations of normal corneas. The term 2 exp(-1/2) is subtracted off since we chose the wavefront height to be zero at the origin (W=0 at x=y=0) in all of our examples.

Around the symmetry axis (at x = 1 mm) this wavefront can be expanded as:

$$W(x, y) = 2[(1- \exp(-1/2) - ((x - 1)^2 + y^2)/2 + ((x - 1)^2 + y^2)^2/8] + \text{higher order terms} \quad (3)$$

The constant terms give the height of the peak of the Gaussian. The quadratic terms correspond to the paraxial spherical wave with a 500 mm radius of curvature. There are no cylinder or cubic (coma) terms present around the symmetry axis. The fourth order terms include spherical aberration.

Around the original axis (x=y=0), the wavefront of Eq. 2 can be expanded as:

$$W(x, y) = 2 [\exp(-r^2/2) \exp(x) -1] \exp(-1/2) \quad (4)$$

$$= K [(1 - r^2/2 + r^4/8 + \ldots)(1 + x + x^2/2! + x^3/3! + x^4/4! + \ldots) -1] \quad (5)$$

$$= K [x - y^2/2 + (x^3/3 - x\, r^2)/2 + (x^4/24 + x^2\, r^2/4 + r^4/8) + \ldots] \quad (6)$$

where $K = 2 \exp(-1/2) = 1.2131$ and $r^2 = x^2 + y^2$.

We can identify the various terms as follows:

paraxial spherical aberration: $K(x^4/24 + x^2\, r^2/4 + r^4/8)$ (7a)

paraxial coma: $-K (x^3/3 + xy^2/2)$ (7b)

paraxial sphero-cylinder: $-Ky^2/2$ (7c)

paraxial prism: Kx (7d)

paraxial piston (offset at origin): 0 (7e)

Eq. 6 can be rewritten as a Zernike expansion. In the limit of an infinitesimal pupil of radius R, the first two terms of Eq. 6 become:

$$W(x, y) = 1.2131(Z_{0,0}\, R^2/8 + Z_{1,1} + Z_{2,0}/4 - Z_{2,2}/4) \text{ plus higher order terms} \quad (8)$$

where the Zernike polynomials are: $Z_{0,0} = 1$, $Z_{1,1} = x$, $Z_{2,0} = x^2 + y^2 - 0.5R^2$, and $Z_{2,2} = x^2 - y^2$ (9)

For R = 2.0 mm, the Zernike expansion of Eq. 2 becomes:

$$W(x, y) = -0.482\, Z_{0,0} + 0.470\, Z_{1,1} - 0.209\, Z_{2,0} + 0.091\, Z_{2,2} \text{ plus higher order terms} \quad (10)$$

Line of Sight and Reference Axis

One of the main topics of concern to the present paper is the question of what to do with the prism term ($0.470\, Z_{1,1}$ for the 4 mm diameter pupil of Eq. 10). This is the question of how to choose the reference axis. A task force sponsored by the Optical Society of America has recommended that the line of sight (LOS) be used as the reference axis.[1] The LOS is the line from the pupil center to the fixation point.

For the reference axis direction let us first consider the case of a large pupil with two extremes for the entering beam: double-pass with incoming rays filling the full pupil, and one-and-a-half-pass (1.5 pass) with a small incoming beam. For a double-pass instrument the LOS would coincide with the coordinate axis we have been using in Eqs. 2 to 10. The incoming rays would be aligned with the fixation point on the z axis. Because the pupil is large, the small Gaussian bump would be negligible, so most of the emerging rays will go back in the z direction. The coordinate system used in Eq. 2 is thus excellent. The wavefront in this coordinate system is shown as the dark curve in Fig. 3a. Now consider the 1.5-pass method that is actually used in Shack-Hartmann measurements.[2] In order to have the retinal image unaffected by unknown aberrations, it is typical to have the entering beam be narrow, on the order of 1 mm in diameter. We assume this beam is coming through the center of the pupil, which is taken to be at x=y=0. This is the chief ray. The beam focuses on the retina and then emerges through the full pupil. The emerging ray coming through the pupil center will retrace the path of the incoming ray (reversibility of light) and would hit the fixation point. The peripheral rays would be skewed off axis. The coordinate system in this case is shown in Fig 3b, where the wavefront is tilted from the case in Fig 3a. The wavefront normal at the pupil center is aligned with the z-axis and the chief ray. The amount of rotation needed in going from 3a to 3b is given by the prism term in Eqs. 6 or 8 (assuming the 1 mm diameter entrance beam is close to 0 mm). This rotation is 1.2131 milliradians (mrad) = .12131 prism diopters = 4.17 min, using 57.3*60/1000= 3.438 min/mrad. For the more realistic case of a 4 mm diameter pupil a rotation of 0.137 mrad maximizes the Strehl ratio for light whose wavelength is 0.5 μm. For a 4 mm pupil and a large wavelength the Gaussian bump aberration becomes relatively small and we enter the regime where the Strehl ratio is well approximated by the wavefront variance[3]:

$$\text{Strehl} = 1 - \text{var}(W)\, (2\pi/\lambda)^2 \quad (11)$$

In this regime the Strehl ratio is optimized by eliminating the Zernike prism term. From Eq. 10 it is seen that a rotation of 0.482 mrad produce a LOS reference axis with vanishing Zernike prism. In summary, we have discussed four possible methods for defining the LOS reference axis in terms of the wavefront W(x, y) in Eq. 2:

Large pupil LOS (double-pass):

$$W_{large}(x, y) = W(x, y) \quad (12a)$$

Small pupil LOS (1.5-pass):

$$W_{small}(x, y) = W(x, y) - 1.183\,x \quad (12b)$$

2 mm pupil LOS, large λ (no Zernike prism):

$$W_{2Z}(x, y) = W(x, y) - 0.470\,x \quad (12c)$$

2 mm pupil LOS, λ = 0.5 (optimal Strehl):

$$W_{2S}(x, y) = W(x, y) - 0.137\,x \quad (12d)$$

Each of the expressions for the wavefront in Eq. 12 corresponds to using the LOS under different viewing conditions. In Figures 1a and 1b, we show that even though the rotations in Eqs. 12 are small (the largest, in Eq. 12b, is 4.17 min) the wavefront takes on a different appearance after the rotation. We contend elsewhere (see discussion of Figs 2a,b for an abbreviated version) that this small difference can also lead to different conclusions regarding visual performance.

The figure shows five different representations of aberrations (rows 1, 2, 4, 5 and 6) for five wavefront shapes (the columns). The columns are the following shapes:

Column 1: Eq. 6 with all the terms (Eq 12a)

Column 2: Eq. 6 minus the paraxial prism term (Eq. 12b)

Column 3: Eq. 6 minus the shifted spherical term, $K((x - 1)^2 + y^2)/2$

Column 4: Eq. 6 minus all terms less than cubic order (the terms shown in Eq. 8)

Column 5: Eq. 1 from the Walsh and colleagues[4]

The rationale for the various manipulations of the lower order terms in the first four columns is as follows. The first column is the original wavefront (Eq. 12a) that has full symmetry around the shifted axis (at x = 1 mm). In the second column the paraxial prism is removed by a rotation of 4.17 min around the y axis. The gray curve in Fig. 3a shows that the slope is 4.17 min at the origin. The third column removes the paraxial prism by removing just the right amount of displaced sphere so no rotation is needed. Finally, the fourth column removes all the second-order terms, leaving only the aberrations. A similar strategy was used by Walsh and colleagues[4], shown in the fifth column for the wavefront of Eq. 1. The third and fourth columns correspond to different strategies for choosing a reference surface. Which of the various options for choosing the reference surface is best depends on the application (determining optimal refractive surgery ablation vs. predicting best uncorrected acuity vs. predicting best corrected acuity).

Five Pupil-based Representations of Aberrations

1. Wavefront elevation—The first representation (Fig. 1) is the standard wavefront contour plot. Contour lines at -2, -1, 0, 2, and 6 μm are shown as indicated by the colorbar legend on the right. In all of our examples we choose the piston term so that the wavefront height at the origin is 0. In our contour plots, values that are more negative than the colorbar range are represented by white. Values that are more positive than the colorbar range are represented by the darkest color of the colorbar. The wavefront representation is especially relevant for refractive surgery since W(x, y)/(n-1) is close to the amount of cornea to be ablated[5], where n is the corneal index of refraction (one must account for epithelial regrowth and corneal reshaping in planning the surgery, and one must choose an optimal reference axis and reference surface, the topic of this paper).

2. Wavefront slope. Acuity Map—The second representation of aberrations (Fig 2) is our novel approach, and is an acuity map since it shows the pupil point spread function (pPSF). It can be thought of as the image space retinal PSF brought to object space and referenced to the pupil plane. The pPSF is given by the wavefront slope:

$$pPSF(x, y) = 3.438 * \text{magnitude}(\text{grad}\,(W(x, y))) \quad (13)$$

where the 3.438 min/mrad conversion was discussed earlier, and the gradient of W is a vector given by:

$$\text{grad}(W) = (dW/dx, dW/dy) = -2\,(x-1, y)\,W(x, y) \text{ for the Eq. 2 wavefront} \quad (14)$$

The quantity in Eq. 14 is the slope of the object space ray at pupil location (x, y) that came from a fixed retinal point. It is precisely the slope being measured by a Shack-Hartmann sensor, the angle between the wavefront normal and the reference axis. Since it is close to the raw data it is fairly independent of wavefront reconstruction assumptions.

The pPSF is probably the most clinically relevant of all the pupil plane representations since it directly shows the blurring in minutes of arc in object space. The lightest shading of gray shows the regions of the pupil in which the blur is less than

one minute. This is the region contributing to 20/20 acuity. Figures 1 and 2 show that the representations of aberrations depend on what is chosen as the reference axis and the reference surface. Panels a-d are representations of the same waveform, yet they look different from each other.

Figure 3 shows horizontal cuts of Figure 1 (black) and Figure 2 (gray) along the x axis. These plots simultaneously show the aberration with the wavefront height (Fig 1) in microns and the point spread function (Fig 2) in minutes.

3. Wavefront slope. The Tscherning "Aberroscope Grid"—Our second representation was a contour plot of the magnitude of the wavefront slope. There are other ways to represent a slope. One could place short arrows at an array of pupil samples.[6] The length of the arrow would be given by Eq. 13 and the direction would be the direction of the slope. Although this can be a useful representation it is often difficult to discern the direction of the arrows and the picture can get cluttered. An alternative is to connect the tips of the arrows making a grid. That is our third representation (Fig 4). It is similar to the representation that Howland and Howland[7] used for their crossed-cylinder aberroscope. It is even closer to the Tscherning[8] aberroscope (using a plus lens rather than a cross-cylinder). The main difference is that our representation is in object space whereas Tscherning's was in image space, on the retina. Our intersection points are similar to an object space spot diagram.

4 and 5. Wavefront Curvature (Refractive Power)—Figures 5 and 6 are two representations of the curvature of the wavefront. Since the wavefront slope (Fig 2) is so small, the curvature is simply the second derivative, to an excellent approximation. To specify the wavefront curvature, one begins by taking three second derivatives of the wavefront: $W_{xx} = d^2W/dx^2$, $W_{yy} = d^2W/dy^2$, $W_{xy} = d_2W/dxdy$. These second derivatives are components of refractive power of the incoming waveform needed to produce a good focus.

There are quite a few ways to combine the three second derivative maps to get integrated power maps:

—Mean curvature, or Laplacian, or equivalent sphere: $ES = (W_{xx} + W_{yy})/2$

—Jackson cross cylinder at 0, $J_0 = (W_{xx} - W_{yy})/2$. This is the coefficient of the small pupil Zernike $Z_{2,2}$ term.

—Jackson cross cylinder at 45, $J_{45} = W_{xy}$. This is the coefficient of the small pupil Zernike $Z_{2,-2}$ term.

—Total Jackson cylinder, $J = \mathrm{sqrt}(J_0^2 + J_{45}^2)$. This is half the usual cylinder.

—Maximum and minimum curvatures = ES + J and ES - J

—Meridional curvature. The component of curvature in the meridional direction.

Several of these representations are already familiar from methods used to represent corneal topography information. Barsky, Klein, and Garcia [6] showed a number of representations for a keratoconic cornea. They described meridional curvature (they called it instantaneous curvature) and mean curvature (close to their Gaussian curvature). They showed how cylinder could be illustrated as short oriented lines on the mean curvature plot. For Figures 5 and 6 we chose to illustrate a different wavefront curvature (also called refractive power since we are discussing the refracted wavefront): maximum and minimum curvature. We found maximum and minimum wavefront curvatures to be especially useful for displaying refractive powers after refractive surgery.

RESULTS

The right-hand column of Figures 1 to 7 are representations of the wavefront presented in Figure 2 of Walsh and coworkers.[4] Our Figures 1e and 4e correspond to their Figures 2c and 2b, respectively. Our inner contour line shows where the wavefront is between -1 and 0 μm and the middle zone is the region between 0 and 2 μm. The negative values are caused by the presence of coma. Panel 2e shows that there is a region with a diameter of around 4 mm where the amount of blur is less than 1 min. The finding that the various panels in 1e to 7e are fairly symmetric around the origin indicates that coma is probably fairly small for this individual. In fact, as seen in Table 3 of Walsh and colleagues[4], observer PD has the smallest amount of coma of their 11 observers. Plot 5e of maximum curvature shows there is a region with about a 4 mm diameter where the maximum curvature is less than 1 diopter. Plot 6e of minimum curvature has a central region that is negative, due to the comatic contribution. However, as seen in Figure 7e, this negative curvature is very close to 0.

Panels a to d are all for the same Gaussian wavefront described by Eqs. 2 to 10. The different columns all have identical Taylor expansion terms above second order. They differ by what is done with the direction of the reference axis (the amount of prism) and what is done with the sphero-cylindrical correction. Panels d are the representations that are similar to what Walsh and colleagues[4] did, namely remove all the Taylor expansion terms below third order. We contend that this may not be the optimal

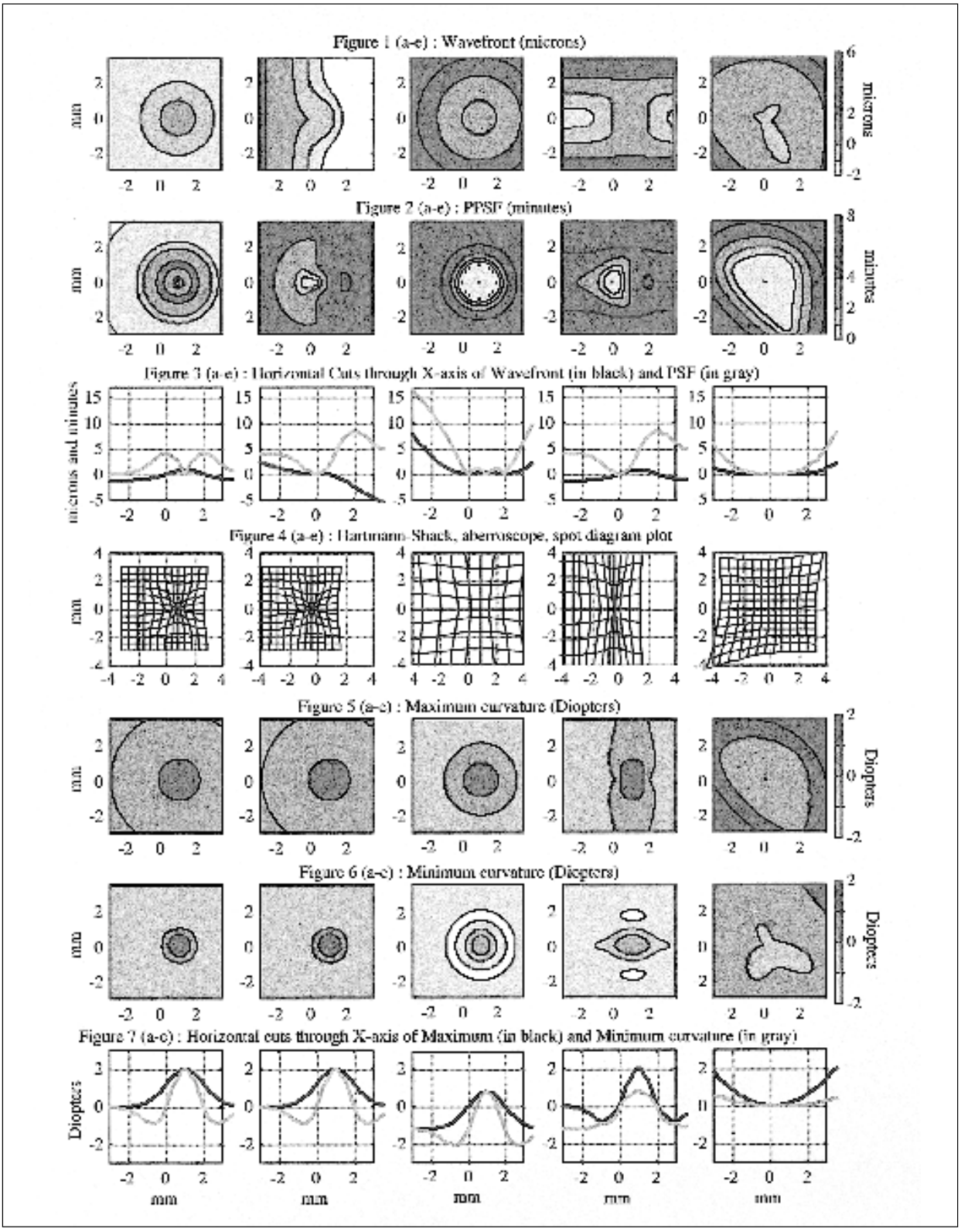
Figure 1 (a-e) : Wavefront (microns)
mm
microns
Figure 2 (a-e) : PPSF (minutes)
mm
minutes
Figure 3 (a-e) : Horizontal Cuts through X-axis of Wavefront (in black) and PSF (in gray)
microns and minutes
Figure 4 (a-e) : Hartmann-Shack, aberroscope, spot diagram plot
mm
Figure 5 (a-e) : Maximum curvature (Diopters)
mm
Diopters
Figure 6 (a-e) : Minimum curvature (Diopters)
mm
Diopters
Figure 7 (a-e) : Horizontal cuts through X-axis of Maximum (in black) and Minimum curvature (in gray)
Diopters
mm

way to view the aberrations or their effect on vision.

The left-hand panels (column a) represent the original Gaussian wavefront. The Gaussian shape of the wavefront is most easily discerned in panel 1a. One of the most instructive pictures for assessing the expected visual quality is Figure 2. Panel 2a shows that there is a large outer ring (the region greater than 2 mm from the center of the Gaussian) where the blur is less than 1 min. We would expect this individual to have quite good vision for a dilated pupil because of the large outer region with minimal blur. The gray line in Figure 3 showing a horizontal cut through the middle of Figure 2 may be an easier way to gain an appreciation for what the contour lines of Figure 2 are representing. The spot ("spider-web") diagrams of Figure 4 are based on the same gradient information used to construct Figure 2. The enlargements that are seen in panels 4c and 4d are due to the removal of sphere (in 4c) and sphero-cylinder (in 4d). The Figure 4 representation provides a quick view (for experienced "spider-web" interpreters) of the Shack-Hartmann raw data and the nature of the aberrations. Figures 5 and 6 have the advantage that because they are second derivatives, they are independent of the prism term. The shape of the contours are also independent of a constant spherical term ($Z_{2,0}$) that merely elevates the plot by a constant. For a cornea after refractive surgery, maximum and minimum curvature (Figs 5, 6) will tend to be the curvature in the radial and tangential directions respectively, relative to the center of the ablation, even for decentered ablations. This robustness of curvature gives it extra reliability. The problem with curvature is that being a second derivative, it will tend to be noisier than the height or slope.

DISCUSSION

Panels a and b of Figures 1 to 3 show that a tilt (rotation) of the reference axis by just 4.17 min makes dramatic changes in the wavefront height (Fig 1) and slope (pupil PSF, Fig 2). Panels a and b use a line of sight (LOS) reference axis for a large pupil double-pass (Eq. 12a) and one-and-a-half-pass (Eq. 12b) instrument, respectively. This shows the LOS does not unambiguously determine a reference direction for viewing aberrations. When the aberrations are small compared to the wavelength of light the wavefront variance is directly related to the physical optics PSF height (Strehl ratio in Eq. 11) and the Strehl ratio is maximized by choosing an axis that removes the Zernike prism (Eq. 12c). For large aberrations the physical optics Strehl ratio is maximized by a rotation (Eq. 12d) that is close to the large pupil rotation (Eq. 12a).

The usual method for representing aberrations at the pupil plane is to show a contour map of the wavefront. In this paper we showed two additional representations based on the wavefront slope and two based on the wavefront curvature. When the aberrations are small the wavefront height gives the best measure of image quality. For large aberrations, geometric optics and wavefront slope (the pupil PSF, Fig 2) gives the best insight into image quality.

Just as the choice of reference axis and sphero-cylindrical reference surface are relevant for how to display the aberrations, they are also relevant for how much cornea to ablate in refractive surgery. A judicious choice of these quantities can result in a residual optics with extended depth of focus with less cornea being ablated than would be the case for a "more obvious" choice of axis and residual refraction.[5]

REFERENCES

1. Applegate RA, Thibos LN, Bradley A, Marcos S, Roorda A, Salmon TO, Atchison DA. Reference axis selection: a subcommittee report of the OSA working group to establish standards for the measurement and reporting of the optical aberration of the eye. In Vision Science and Its Applications, OSA Technical Digest (Optical Society of America, Washington DC) 2000:146-149.
2. Liang J, Williams DR. Aberrations and retinal image quality of the normal human eye. J Opt Soc Am A 1997;14: 2873-2883.
3. Marachal A. Rev d'Optique 1947;26:257.
4. Walsh G, Charman WN, Howland HC. Objective technique for the determination of monochromatic aberrations of the human eye. J Opt Soc Am A 1984;1:987-992.
5. Klein SA. Optimal corneal ablation for eyes with arbitrary Hartmann-Shack aberrations. J Opt Soc Am A 1998;15:2580-2588.
6. Barsky BA, Klein SA, Garcia DD. Gaussian power with cylinder vector field representation for corneal topography maps. Optom and Vision Sci 1997; 74:917-925.
7. Howland B, Howland HC. Subjective measurement of high-order aberrations of the eye. Science 1976;193:580-582.
8. Tscherning M. Die monochromatischen abberationen des menschlichen auges. Z Psychol Physiol Sinn 1894;6:456-471.